

Far-field Radiative Thermal Rectification with Bulk Materials

Sreyash Sarkar*, Elyes Nefzaoui†, Philippe Basset, and Tarik Bourouina

ESYCOM, Univ Gustave Eiffel, CNRS, CNAM, ESIEE Paris,
F-77454 Marne-la-Vallée, France

July 24, 2020

Abstract

In this paper, we explore the far-field radiative thermal rectification potential of common materials such as metals, dielectrics and doped semiconductors using radiative and thermo-radiative properties extracted from literature. Ten different materials are considered. The rectification coefficient is then calculated for 44 pairs of materials; each pair can be used for the two terminals of a radiative thermal diode. A thermal bias of 200 K is considered. The choice of materials and thermal bias value are only bound by data availability in literature. Obtained results, highlight new candidate materials for far-field radiative thermal rectification. They also highlight materials where thermal rectification is not negligible and should be considered with care in heat transfer calculations when considering systems subject to a comparable thermal bias and where these materials are used. Among the materials studied, undoped Indium Arsenide (InAs) shows great promise to be employed for thermal rectification, with a thermal rectification ratio reaching 90.5% in combination with other materials. Obtained results pave the way for an optimized design of thermal radiation control and management devices such as thermal diodes.

1 Introduction

Thermal rectification (TR) can be defined as an asymmetry in the heat flux when the temperature difference between two interacting thermal reservoirs is reversed. Therefore, a two-terminal thermal device exhibits thermal rectifi-

*corresponding author: sreyash.sarkar@esiee.fr

†corresponding author: elyes.nefzaoui@esiee.fr

cation if it transports heat in one direction with more ease than in the reverse direction. Thermal rectification has been a subject of intrigue since its underlying test perception in 1936 by Starr [1] because of its aptitude to open up innovation in heat transport control, inspiring analogies to the tremendous advancement in the electronics industry following the invention of such nonlinear elements as the transistor and the diode. Other potential applications of thermal rectification include thermal barrier coatings [2], enhanced efficiency thermoelectric devices [3, 4], or temperature variation driven heat engines[5]. From that point forward, several investigations have been performed to understand which systems can exhibit thermal rectification[6] and have introduced the concepts of numerous innovative devices like thermal transistors [7–10], thermal logic circuits[11–15] and thermal diodes[16–21]. Recent investigations of thermal rectification have covered different heat transfer(HT) modes including conduction [22, 23], convection [24] and radiation [25–32]. We describe the main current trends in the following paragraphs and more extensive reviews can be found in [6, 33].

To achieve conductive thermal rectification, several mechanisms have been proposed including thermal potential barrier between material contacts[25], thermal strain/warping at interfaces of two materials[26], nanostructured geometric asymmetry[34] and anharmonic lattices[29]. The asymmetry at the interface between two materials due to the difference of their thermal conductivity temperature dependence has also been shown to be the main driving mechanism for conductive thermal rectification by Marucha et. al[35] and subsequently used in the models of Hoff et. al[36], Sun et. al[37] and in Go et. al[38]. Based on the same principle, Hu et al[39] and Zhang et. al[22] presented thermal rectifiers based on different thermal conductivities of dissimilar graphene nano-ribbons or Y junctions. At the micro and nano-scales, the asymmetry at the origin of TR can be widely tuned and engineered in nanostructured materials [40] which led to many contributions using several phenomena observed in a large diversity of nano-structures such as ballistic phonons anisotropy at large thermal bias [2], phonons lateral confinement[41] and the temperature dependence of lattice vibrations density of states[42]. Solid-state thermal rectifiers have also been proposed taking benefit of nonlinear atomic vibrations[29][43], nonlinear dispersion relations of the electron gas in metals[44], and thermal streams through Josephson junctions[45] or metal-superconductor nano-intersections[46]. At even smaller scales, TR in quantum systems has recently lured researchers such as in the work of Landi et.al[47] on TR using a quantum XXZ chain subject to an inhomogeneous field and the research of Chi et. al [47] discussing TR in a system of a single level quantum-dot connected to ferromagnetic leads. On the other hand, Scheibner et al[48] experimentally demonstrated a TR behavior in quantum dots subject to high in-plane magnetic fields[48] and most recently in the work of Senior et. al[49], it has been shown that a superconducting quantum bit coupled to two superconducting resonators can achieve magnetic flux-tunable photonic heat rectification between 0 and 10%.

Radiative heat transfer is another heat transfer mode that has been actively investigated for thermal rectification application in the past decade after the seminal works of Ruokola et. al[50] and Otey [30]. Two main paths have been considered. On one hand, near field (NF) Radiative Thermal Rectification (RTR) between materials supporting resonating surface waves separated by wavelength scale or sub-wavelength gaps. Plasmonic materials supporting surface plasmon polaritons and dielectrics supporting surface phonon polaritons have been mainly considered. Used materials for NF RTR include gold and silicon [51, 52] with temperatures between 300K and 600K, doped silicon[53], SiC [30, 31, 54], SiC and SiO₂ [32, 55], InSb and graphene-coated SiO₂[56]. Many works on NF RTR also used phase change materials and mainly Vanadium Dioxide (VO₂)[57–60], and more rarely, thermochromic materials [61]. In addition to the diversity of used materials, a large variety of geometries and sizes has been explored as in the work of Shen et. al[34], which elucidated non-contact thermal diodes using asymmetric nanostructures while [62, 63] reported on Near field RTR in the deep sub-wavelength regime between planar surfaces separated by nanometre-scale distances. Zhou et. al[64] proposed for instance a thermal diode using a nanoporous plate and a plate, both made of silicon carbide and where the two terminals are separated by a nanometric vacuum gap while Ott et. al[19] explored a radiative thermal diode made of two nanoparticles coupled with the nonreciprocal surface modes of a magneto-optical substrate.

On the other hand, far-field (FF) radiative heat transfer also enables RTR and has been an active area of interest in the past decade. Compared to NF RTR, FF RTR provides the advantage of simplicity and ease of fabrication since it does not require the combination and alignment of objects separated by micro-metric or nano-metric gaps. Two main solutions have been reported for this purpose : the use of phase change materials (PCM) [9, 18, 65] and tunable meta-materials often used as selective radiation emitters and absorbers[66]. The use of phase change materials, and VO₂ in particular, is predominant in both conceptual [67] and experimental works [68, 69]. Recently, Ghanekar et. al[70] proposed the concept of a far-field radiative thermal rectifier combining both PCM, VO₂ for instance, and a Fabry-Perot cavity based meta-material. Beyond thermal rectification, various radiative heat transfer control devices have been proposed such as thermal transistors [7–10, 71] and photonic thermal memristors [72]. The large majority of those PCM based far-field radiation control devices use VO₂ since the seminal work of Van Zwol et. al[73] who provided a comprehensive characterization of VO₂ radiative and thermo-radiative properties (TRP) around its metal-insulator transition temperature. Surprisingly, the good performances of VO₂ for RTR seem to have prevented authors from exploring other materials, contrarily to the what have been done and reported for NF RTR. Indeed, the large variety of existing materials have not been systematically considered to assess their potential use in FF RTR. This can be legitimately explained by the scarcity of literature on materials' radiative properties in the wavelength range of interest for thermal radiation and their subsequent temperature dependence. However, a thorough investigation of commonly avail-

able materials performances with respect to thermal rectification has not been realized up until now.

In the present work, we present an evaluation of RTR potential of different materials commonly used in micro-fabricated devices such as Indium Arsenide, Gallium Arsenide, Gallium Antimonide, Germanium, Zinc Sulphide, Silicon and metals such as Copper and Gold based on radiative and thermo-radiative properties available in literature. The paper is organized as follows: in the present section, we introduce the concept of thermal rectification along with a brief review of the works accomplished so far and delineate the pertinence of the present work; next in section 2, we explain the principle of radiative thermal rectification and introduce the main quantities that govern and characterize a radiative thermal rectification behavior. We also, describe the used radiative and thermo-radiative properties of the considered materials and the process of relevant data extraction from literature. Finally, we report and discuss the main results on the radiative thermal rectification potential of the considered materials in section 3.

2 Methods

2.1 Theory

Variation of the heat flux magnitude when the sign of the temperature gradient between two points is reversed is the basic definition of thermal rectification. Let us consider two thermal reservoirs 1 and 2 at two different temperature T_1 and T_2 , respectively, with $T_2 > T_1$. The temperature difference between the two reservoirs is noted $\Delta T = T_2 - T_1$. This temperature difference results in heat flux Φ_F . We will refer to this initial configuration as forward bias configuration. If we invert the temperature difference between the two reservoirs, i.e if we set reservoir 1 temperature to T_2 and reservoir 2 temperature to T_1 , a reverse bias flux Φ_R is observed. Thermal rectification occurs when the heat fluxes in forward Φ_F and reverse bias Φ_R , under the same magnitude of the thermal potential difference, i.e for a constant $|\Delta T|$ but with opposite ΔT signs, are unequal. Thermal rectification is generally quantified, even though it is not the only indicator encountered in the literature, by means of the normalized rectification coefficient [1, 6] which can be defined as:

$$R = \frac{|\Phi_F - \Phi_R|}{\max(\Phi_F, \Phi_R)} \quad (1)$$

where, Φ_F and Φ_R denote the heat flux under forward and backward bias, respectively. In this paper, the definition of normalized rectification coefficient given in equation 1 is preferred because it provides bound rectification coefficient values between zero and one, as opposed to alternative definitions adopted

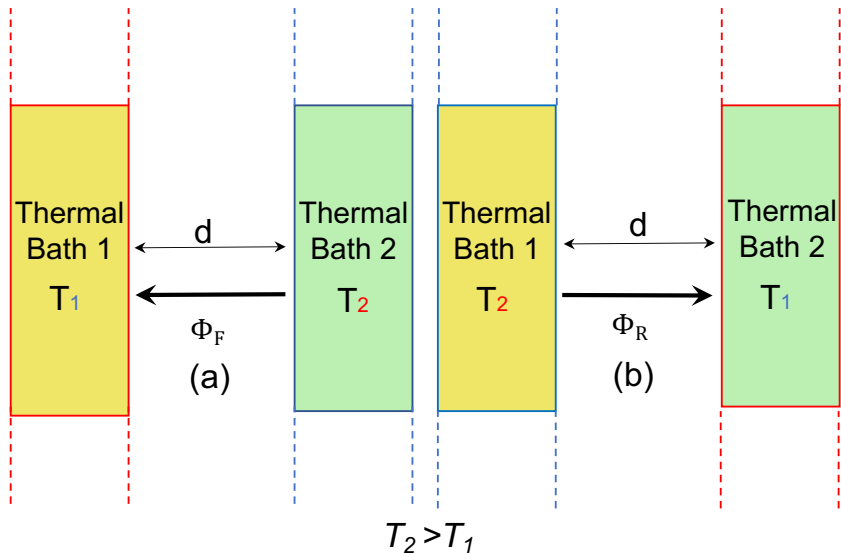


Figure 1: (a) Forward and (b) Reverse bias conditions of HT between two semi-infinite planes acting as thermal baths separated by a vacuum gap of thickness, d . Thermal rectification occurs only when, Φ_F and Φ_R denoting the heat flux in the forward and reverse operating modes under two temperatures ($T_2 > T_1$), are unequal. The gap width (d) is assumed to be much larger than the dominant thermal radiation wavelength (Wien wavelength, $\lambda_W(T)$).

by some authors[46, 74] which lead to values from zero to infinity. A schematic of two thermal reservoirs exchanging heat flux in forward and reverse bias configurations is given in 1.

In this paper, we consider the simple case of far-field radiative thermal rectification between two semi-infinite planes, separated by a vacuum gap of thickness d , characterized by their radiative optical properties (their temperature dependent emissivities and reflectivities). Therefore, the distance separating the two planes exchanging heat by radiation is much larger than the characteristic wavelength of thermal radiation at the considered bodies temperatures given by Wien's law : $d > \lambda_W(T)$, where $\lambda_W(T) = \frac{hc^2}{5k_B T}$, where h , c , k_B and T are Planck's constant, the speed of light in vacuum, Boltzmann constant and the absolute temperature respectively. For simplicity's sake, we also assume they are both Lambertian sources, meaning that their emissivities and reflectivities ($\epsilon(\lambda, T)$ and $\rho(\lambda, T)$ respectively) are direction independent[75]. Considering these assumptions, the net radiative heat flux (RHF) exchanged by the two bodies resumes then to the far field contribution, which can be written

as[55]:

$$\Phi(T_1, T_2) = \pi \int_{\lambda=0}^{\infty} [I^0(\lambda, T_1)I^0(\lambda, T_2)]\tau(\lambda, T_1, T_2)d\lambda \quad (2)$$

where,

$$I^0(\lambda, T) = \frac{hc^2}{\lambda^5} \frac{1}{e^{\frac{hc}{k_B T}} - 1} \quad (3)$$

is the black body intensity at a temperature T and wavelength λ , where h , c , k_B and T are Planck's constant, the speed of light in vacuum, Boltzmann constant and the absolute temperature respectively[76] and

$$\tau(\lambda, T_1, T_2) = \frac{\epsilon(\lambda, T_1)\epsilon(\lambda, T_2)}{1 - \rho(\lambda, T_1)\rho(\lambda, T_2)} \quad (4)$$

is the monochromatic RHF density transmission coefficient between 1 and 2, where $\epsilon(\lambda, T)$ and $\rho(\lambda, T)$ is the monochromatic emissivity and reflectivity at a given temperature respectively. The RHF density transmission coefficient is governed by the radiative properties of the two considered thermal baths, in particular their emissivities and reflectivities and the temperature dependence of these properties. These properties are completely governed by the considered bodies dielectric functions and geometries. In the case of opaque bodies, energy conservation[75] and Kirchoff's laws [75] combination leads to the following relation between the monochromatic emissivity, reflectivity and transmittivity at a given temperature:

$$\epsilon(\lambda, T) = 1 - \rho(\lambda, T) - t(\lambda, T) \quad (5)$$

Therefore, to evaluate the thermal rectification potential of a given pair of materials, we need to know the emissivity, reflectivity and transmittivity of each terminal of the considered thermal diode and its temperature dependence. Since the emissivity and reflectivity depend on the dielectric function, knowing the dielectric permittivity or the complex refractive index of the considered materials is also sufficient to estimate their potential for thermal rectification. In our case, these data have been harvested from literature.

2.2 Radiative properties data extraction

Thermo-radiative properties, i.e materials radiative properties and their temperature dependence, are the main input data required to assess the radiative thermal rectification ability of a given material. Difficulty to obtain such data, especially in the wavelength range of thermal radiation from room temperature to a few hundred Kelvins above room temperature, i.e. in the mid and far-infrared, perhaps explains the dearth of literature on thermal rectification with the large variety of existing materials and the strong concentration of literature on VO_2 . Although the most important material libraries in this regard

such as The Handbook of Optical Materials by Edward D. Palik [77] and that of Weber[78], provide an exhaustive collection of material optical properties, unfortunately, available data is not temperature dependent. Radiative properties of common materials at different temperatures, in the required infrared range, are scantily available in literature. Incidentally, the majority of relevant data found, regarding the works dedicated to this sub-area of research, are pertaining to the study of semiconductors. The optical properties of metals such as, Gold [79, 80], Aluminum [81, 82], Tungsten [80], Molybdenum[83], Silver [84], Copper [85], Nickel [85] have been studied, but unfortunately researchers have not been particularly interested in exploring the aforesaid optical properties at higher temperatures and at larger wavelengths, adherent to the IR range, which is an imperative in this study. Materials like Si [31] and Ge [86] have been considered broadly, beginning in the 1950's. GaAs, InAs, InP, and GaSb make a case for volumes of research of their own and have been utilized as a part of light emanating and optoelectronic devices [87]. Material properties were learned at temperatures extending from low temperatures (liquid helium, 4.2 K, or liquid nitrogen, 77 K) to about room temperature, 298 K [87]. The 2010 work of Thomas R. Harris [87] provides valuable experimental data on the study of optical properties of Germanium, Gallium and Indium derivatives and on Bulk Silicon, at various temperatures. Optical properties of Silicon Carbide [88, 89], and on Zinc Sulphide [90] have also been reported in the past decades. The use of numerical simulation data for bulk silicon generated using a Drude Model was also suggested in [91, 92], and we took use of this model to produce temperature dependent radiative properties data for bulk silicon. The list of materials considered in the present study is indicated in Table 1.

Table 1: Considered Materials

Materials	Symbols
Germanium[87, 93]	Ge
Gallium Derivatives[87, 94]	GaAs,GaSb
Undoped Indium Arsenide[87, 95, 96]	InAs
Zinc Sulphide [90, 97–99]	ZnS
Silicon Carbide[55, 88]	SiC
Bulk Doped N-type Silicon($1 \times 10^{20} cm^{-3}$)	DBuSi ₁
Bulk Doped N-type Silicon($3 \times 10^{20} cm^{-3}$)	DBuSi ₃
Gold [79, 80]	Au
Copper[85]	Cu

In the work of Thomas R. Harris[87], temperature dependent transmission measurements for Ge were taken up to approximately 650 K. The data was taken in near IR and mid IR wavelength ranges. Comparison with older literature[100] shows good agreement, indicating that the measured data are reliable. Similarly, temperature dependent transmission measurements were taken up to approximately 850 K for undoped GaAs and up to approximately

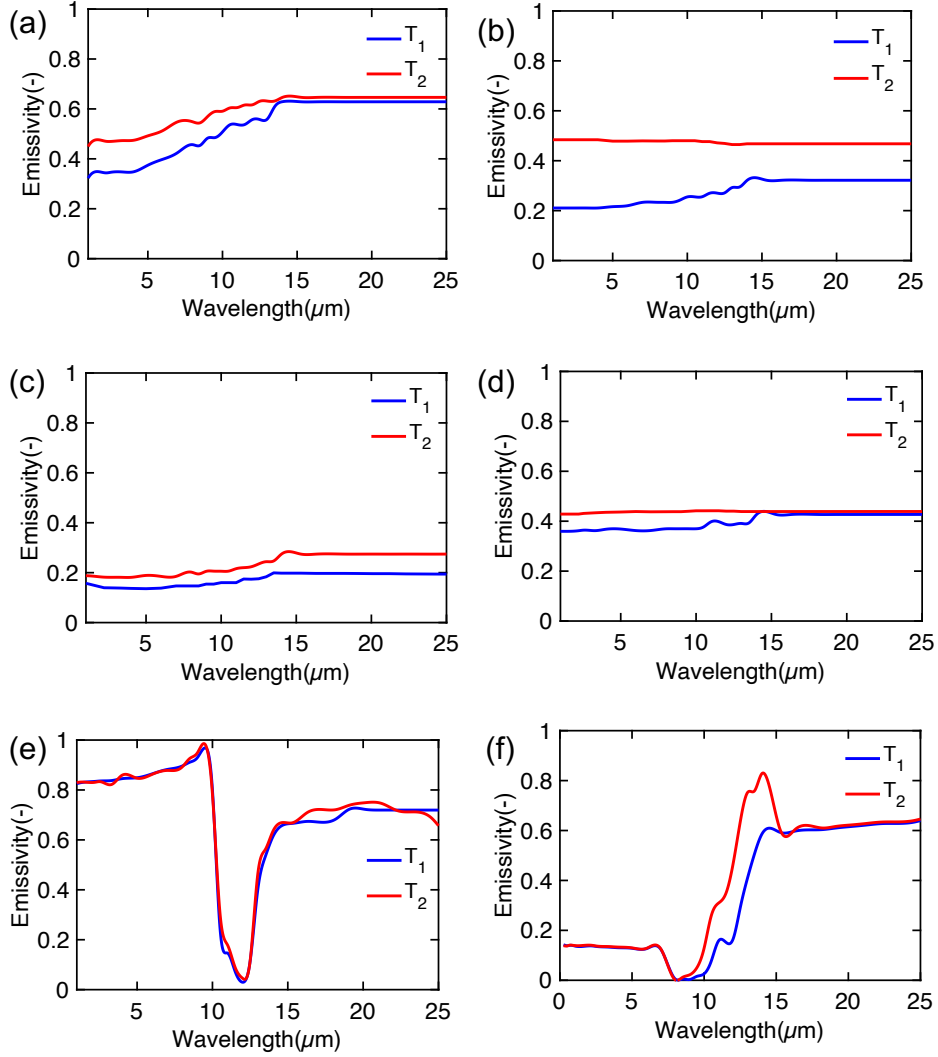


Figure 2: Emissivity of a few common materials found in literature-(a) GaSb (b) InAs (c) GaAs (d) Ge (e) SiC (f) ZnS at $T_1=300\text{K}$ and $T_2=500\text{K}$.

550 K for n-type GaAs doped with silicon. In the case for undoped GaSb, measurements were taken up to 650 K. Unfortunately, for sulphur doped InP, only near IR measurements were reported, which renders the data set incomplete for usage in the present study[87]. Thus, temperature dependent transmission measurements were carried out for Si, Ge, GaAs, GaSb, InAs, and InP from 0.6 to 25 μm at temperatures ranging from 295 up to 900 K. Band gap shifts were observed as temperature changed and were compared to previous works.

General agreement was observed in the trend of the change in the band gap with temperature, however, the actual band gap energy values deviated from the expected-on average by about 10 %. The reflectivity maximum increased in magnitude with increasing temperature, with successful measurements being done up to 517 K[87].

To completely gather temperature dependent reflectivity data of GaAs, GaSb, InAs, Ge another set of works were adhered to such as the work of Skauli et. al[94], where the refractive index of GaAs has been measured. From 1979-1984, H. H Li[93, 97] prepared a comprehensive report on the temperature dependence of the refractive indices of Si, Ge, ZnS, ZnSe, ZnTe etc., where he provided near non-existent temperature-dependent data on these particular semi-conductors refractive index in a wide spectral range including mid and far infra-red.

For SiC in the IR wavelength range from 1 μm to 25 μm , many data are available in literature and because much of SiC optical properties depend on its crystallographic orientation [101, 102], they have been compared to other semiconductor relevant data with care. Some widely citepd sources are that of Bohren et. al [103], Mutschke et al.[104, 105], the measurements of Daniel Ng [88] and Joulain et. al [55]. Cagran et. al[106] provided a comprehensive study on the temperature-resolved infrared spectral emissivity of SiC and this data was finally employed in the present study due to its reportage of wide and flexible temperature dependence of emissivity.

On the other hand, the measurements on Zinc Sulphide (ZnS) reported in [90, 98, 99] provide valuable insight into the thermal, structural and optical properties of a commercially available sample of multispectral ZnS. The hemispherical transmission, reflectivity, absorptivity, emissivity of unpolarized light at normal incidence on ZnS at 24 °C, 100 °C and 200 °C are reported in [90].

3 Results and discussion

A simple Matlab program based on equations 1 to 5, was implemented to quantify the thermal rectification coefficient for different pairs of materials, which takes the reflectivity data-set of two different materials and their temperature as input and calculates the forward and reverse bias fluxes, thereby finally giving the value of RTR coefficient as defined in equation 1. Radiative optical properties of the materials under consideration were studied at a temperature difference of 200 K, with $T_1=300\text{K}$ and $T_2=500\text{K}$ while the spectral range taken into account is 1 - 25 μm . This temperature range was considered under the constraints of data availability.

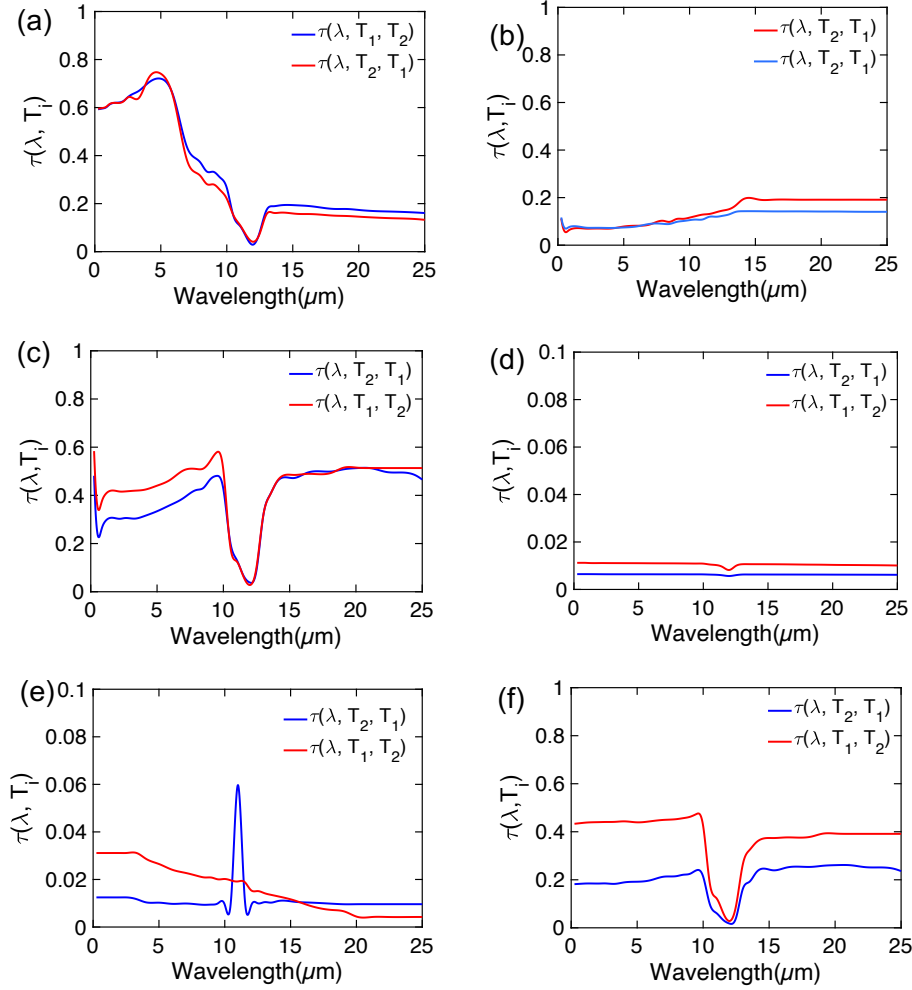


Figure 3: Obtained RHF density transmission coefficients in forward and reverse bias configurations between two materials- (a) SiC/DBuSi($1 \times 10^{20} \text{cm}^{-3}$) ; (b) GaAs/GaSb; (c) SiC/GaSb; (d) SiC/Au; (e) InAs/Cu (f) InAs/SiC at $T_1=300\text{K}$ and $T_2=500\text{K}$.

Table 1 shows the list of materials considered in this study. The respective unequal RHF density transmission coefficients in forward and reverse directions for considered pairs of materials are illustrated in Fig. 3, while Table 4 summarises the obtained RTR coefficient for all possible pairs of materials with 44 pairs of materials considered in this study.

Among the materials under consideration, Indium Arsenide (InAs) shows the largest values of RTR coefficient, up to 90.50% when used with SiC, as

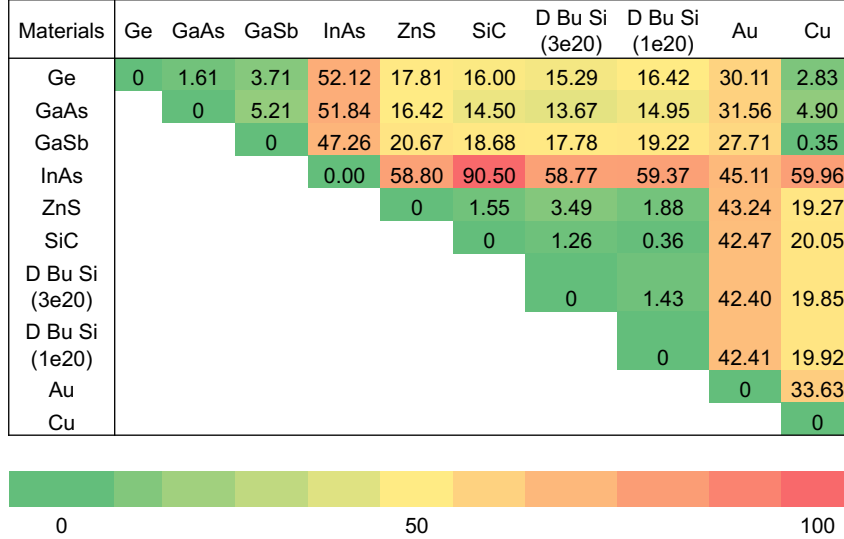


Figure 4: RTR coefficients of thermal rectifiers made of pairs of considered materials for a thermal bias of 200 K.

shown in Table.4. The highest value of RTR with materials other than InAs-SiC, can invariably be attributed to InAs-Cu which records a value of 59.96%. As can be seen in Table.4, all materials in combination with InAs record more than 50% RTR except Au, which has an RTR value of 45.11%. Au, in fact records greater 40% with most materials in the table except Ge, GaAs and GaSb. Au-Ge, Au-GaAs combinations yield an RTR coefficient larger than 30% and so does the metal-metal combination of Au-Cu. All other material combinations depicted in Table.4, fall below 30%. The lowest value of RTR is recorded by a combination of GaSb-Cu and GaSb-DBuSi(1e20)- 0.5 %.

In order to obtain a perfect thermal rectifier, the spectra of the two thermal baths should perfectly match for a given temperature difference, so the exchanged heat flux is maximal, and perfectly mismatch when the thermal gradient is reversed so the exchanged flux is minimized. In fact, in the case of perfectly matching spectra, radiation emitted by one body at any wavelength is absorbed by the second body, while it is completely reflected and returned to the emitter in the case of perfectly mismatching spectra. A perfect one-way heat transmitter, i.e., a thermal diode can then be realised.

We show in Table 5, the normalized RTR coefficient which is defined as a ratio of RTR to the magnitude of the considered thermal potential difference $|\Delta T|$. Note that this definition of normalized RTR enables comparison of different pairs of materials operating under different thermal potential differences. However, this particular definition is not applicable for PCM materials

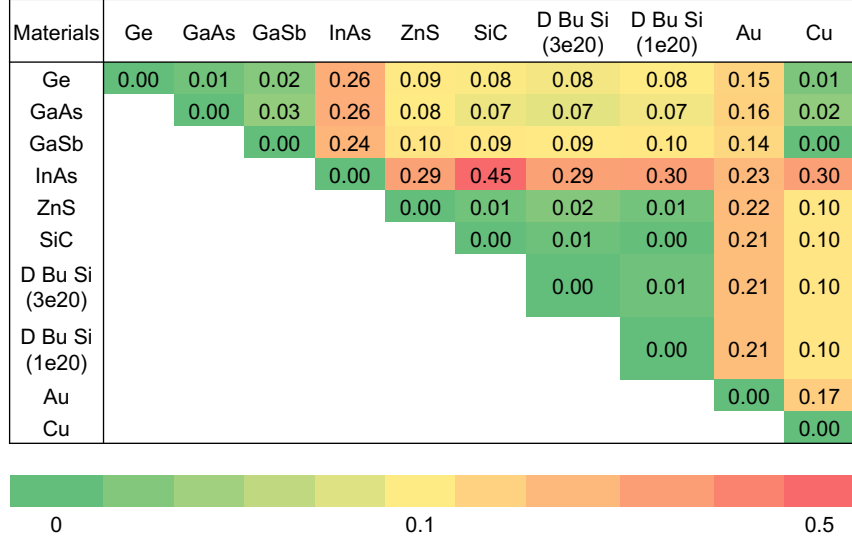


Figure 5: Normalized RTR coefficient i.e RTR coefficients of thermal rectifiers made of pairs of considered materials normalized by the thermal bias.

which exhibit a significant change of their radiative properties with a very small temperature variation around their critical temperature which would lead to an infinite normalized RTR.

In Table 6, we present the Temperature Coefficient of total Emissivity (TCE) that can be defined by $\frac{d\epsilon_t}{dT}$, where, ϵ_t is a spectral average with the spectral emissive power as a weighting factor and can be defined as [75]:

$$\epsilon_t = \frac{1}{n^2 \sigma T^4} \int_0^\infty \epsilon_\lambda(T, \lambda) E_{b\lambda}(T, \lambda) d\lambda \quad (6)$$

where, σ is the Stefan–Boltzmann constant, T is the absolute temperature, $\epsilon_\lambda(T, \lambda)$ is the spectral hemispherical emissivity and $E_{b\lambda}(T, \lambda)$ is the blackbody spectral emissive power. This quantity(TCE) has been defined in a similar manner to the refractive index temperature coefficient, $\frac{dn}{dT}$ commonly used in optics[96]. Here due to data availability constraints, a thermal bias of 200 K was considered. TCE can be used as a key indicator to identify the best candidate materials for thermal rectification since a large variation of radiative properties with respect to temperature is required to obtain a large thermal rectification coefficient. As can be observed in Table 6, the greater the TCE, the more susceptible the materials are for thermal rectification, thus reaffirming the best case of a far field radiative thermal rectifier composed of InAs and SiC. Results reported in the present manuscript could thus serve as red a basic guiding step for researchers and engineers interested in the design of radiative thermal rectifiers for the choice of best candidate materials.

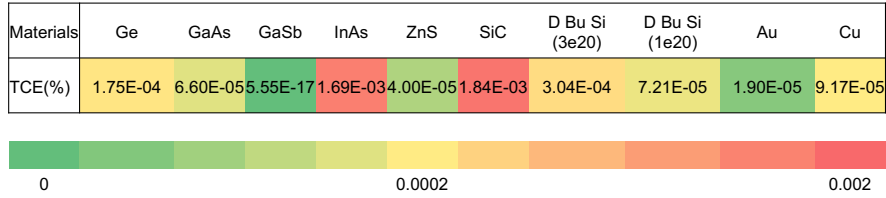


Figure 6: TCE(%) of thermal rectifiers made of pairs of considered materials.

4 Conclusion

We reported in this paper on the thermal rectification potential of 44 pairs of materials commonly used in several applications such as the microelectronics industry. At first, the theoretical concept of thermal rectification is introduced and the key quantities are defined. Then, used radiative properties, a key parameter for RTR coefficients calculation, are presented. Finally, results of the RTR coefficient of 44 pairs of materials are reported. Obtained results show that Indium Arsenide and Silicon Carbide can be very good candidates for a far-field radiative thermal rectifier when combined together with a rectification ratio up to 90.5% for a thermal bias of 200 K. We also show that several pairs of materials provide a relatively high rectification coefficient, larger than 50%. This suggests that they can also be used for thermal rectifiers. A corollary of this result is that non negligible thermal rectification occurs when these pairs of materials are combined in a system with a thermal bias of the order of hundreds of kelvins. Taking into account the temperature dependence of the materials radiative properties is therefore mandatory for an accurate calculation of the exchanged heat flux between these materials in such systems. Presented results may be helpful for thermal management applications and in the advancement of the research and engineering of thermal rectifiers, thermal logical circuits and in thermal energy harvesting.

Acknowledgement

This work was supported by SATT IDF Innov (now Erganeo) in the framework of the project DITHER and by the I-SITE FUTURE Initiative (reference ANR-16-IDEX-0003) in the framework of the project NANO-4-WATER.

References

- [1] Chauncey Starr. The copper oxide rectifier. *Physics*, 7(1):15–19, 1936.

- [2] John Miller, Wanyoung Jang, and Chris Dames. Thermal rectification by ballistic phonons in asymmetric nanostructures. In *ASME 2009 Heat Transfer Summer Conference collocated with the InterPACK09 and 3rd Energy Sustainability Conferences*, pages 317–326. American Society of Mechanical Engineers Digital Collection, 2009.
- [3] Sanjoy Saha, Li Shi, and Ravi S Prasher. Monte carlo simulation of phonon backscattering in a nanowire. In *ASME 2006 International Mechanical Engineering Congress and Exposition*, pages 549–553. American Society of Mechanical Engineers Digital Collection, 2006.
- [4] Giuliano Benenti, Giulio Casati, Carlos Mejía-Monasterio, and Michel Peyrard. From thermal rectifiers to thermoelectric devices. In *Thermal Transport in Low Dimensions*, pages 365–407. Springer, 2016.
- [5] Björn Sothmann, Rafael Sánchez, Andrew N Jordan, and Markus Büttiker. Rectification of thermal fluctuations in a chaotic cavity heat engine. *Physical Review B*, 85(20):205301, 2012.
- [6] Nick A. Roberts and D. G. Walker. A review of thermal rectification observations and models in solid materials. *International Journal of Thermal Sciences*, 50(5):648–662, 2011.
- [7] Jose Ordonez-Miranda, Younès Ezzahri, Jose A Tiburcio-Moreno, Karl Joulain, and Jérémie Drevillon. Radiative thermal memristor. *Physical review letters*, 123(2):025901, 2019.
- [8] Philippe Ben-Abdallah and Svend-Age Biehs. Near-field thermal transistor. *Physical review letters*, 112(4):044301, 2014.
- [9] Karl Joulain, Younès Ezzahri, Jérémie Drevillon, and Philippe Ben-Abdallah. Modulation and amplification of radiative far field heat transfer: Towards a simple radiative thermal transistor. *Applied Physics Letters*, 106(13):133505, 2015.
- [10] Karl Joulain, Jérémie Drevillon, Younès Ezzahri, and Jose Ordonez-Miranda. Quantum thermal transistor. *Physical review letters*, 116(20):200601, 2016.
- [11] Kathmann Christoph, Marta Reina, Riccardo Messina, Philippe Ben-Abdallah, and Biehs Svend-Age. Scalable radiative thermal logic gates based on nanoparticle networks. *Scientific Reports (Nature Publisher Group)*, 10(1), 2020.
- [12] Giulio Casati. Device physics: The heat is on—and off. *Nature nanotechnology*, 2(1):23, 2007.

- [13] Sohail Murad and Ishwar K Puri. A thermal logic device based on fluid-solid interfaces. *Applied Physics Letters*, 102(19):193109, 2013.
- [14] E Nefzaoui, Younès Ezzahri, Karl Joulain, and Jérémie Drevillon. Photonic structures based thermal rectification : Toward tunable radiative thermal rectifiers. In *International Heat Transfer Conference Digital Library*, 2015.
- [15] Christoph Kathmann, Marta Reina, Riccardo Messina, Philippe Ben-Abdallah, and Svend-Age Biehs. Scalable radiative thermal logic gates based on nanoparticle networks. *Scientific Reports*, 10(1):1–11, 2020.
- [16] Maria José Martínez-Pérez, Antonio Fornieri, and Francesco Giazotto. Rectification of electronic heat current by a hybrid thermal diode. *Nature nanotechnology*, 10(4):303, 2015.
- [17] Philippe Ben-Abdallah and Svend-Age Biehs. Phase-change radiative thermal diode. *Applied Physics Letters*, 103(19):191907, 2013.
- [18] Jose Ordonez-Miranda, Karl Joulain, Domingos De Sousa Meneses, Younes Ezzahri, and Jérémie Drevillon. Photonic thermal diode based on superconductors. *Journal of Applied Physics*, 122(9):093105, 2017.
- [19] Annika Ott, Riccardo Messina, Philippe Ben-Abdallah, and Svend-Age Biehs. Radiative thermal diode driven by nonreciprocal surface waves. *Applied Physics Letters*, 114(16):163105, 2019.
- [20] Jose Ordonez-Miranda, James M Hill, Karl Joulain, Younes Ezzahri, and Jérémie Drevillon. Conductive thermal diode based on the thermal hysteresis of vo2 and nitinol. *Journal of Applied Physics*, 123(8):085102, 2018.
- [21] Zhen Chen, Carlaton Wong, Sean Lubner, Shannon Yee, John Miller, Wanyoung Jang, Corey Hardin, Anthony Fong, Javier E. Garay, and Chris Dames. A photon thermal diode. *Nature communications*, 5:5446, 2014.
- [22] Gang Zhang and Haishuo Zhang. Thermal conduction and rectification in few-layer graphene y junctions. *Nanoscale*, 3(11):4604–4607, 2011.
- [23] Tadeh Avanesian and Gisuk Hwang. Adsorption-based thermal rectifier. In *ASME 2015 13th International Conference on Nanochannels, Microchannels, and Minichannels collocated with the ASME 2015 International Technical Conference and Exhibition on Packaging and Integration of Electronic and Photonic Microsystems*. American Society of Mechanical Engineers Digital Collection, 2015.
- [24] A Reis and I Smith. Convective thermal rectification in an air-filled parallelogramic cavity. In *Solar Energy Utilization*, pages 605–617. Springer,

1987.

- [25] GFC Rogers. Heat transfer at the interface of dissimilar metals. *International Journal of Heat and Mass Transfer*, 2(1-2):150–154, 1961.
- [26] AM Clausing. Heat transfer at the interface of dissimilar metals—the influence of thermal strain. *International Journal of Heat and Mass Transfer*, 9(8):791–801, 1966.
- [27] DV Lewis and HC Perkins. Heat transfer at the interface of stainless steel and aluminum—the influence of surface conditions on the directional effect. *International Journal of Heat and Mass Transfer*, 11(9):1371–1383, 1968.
- [28] Nuo Yang, Gang Zhang, and Baowen Li. Carbon nanocone: A promising thermal rectifier. *Applied Physics Letters*, 93(24):243111, 2008.
- [29] Baowen Li, Lei Wang, and Giulio Casati. Thermal diode: Rectification of heat flux. *Physical review letters*, 93(18):184301, 2004.
- [30] Clayton R. Otey, Wah Tung Lau, and Shanhui Fan. Thermal rectification through vacuum. *Physical Review Letters*, 104(15):154301, 2010.
- [31] Mathieu Francoeur, Soumyadipta Basu, and Spencer J. Petersen. Electric and magnetic surface polariton mediated near-field radiative heat transfer between metamaterials made of silicon carbide particles. *Optics express*, 19(20):18774–18788, 2011.
- [32] Hideo Iizuka and Shanhui Fan. Rectification of evanescent heat transfer between dielectric-coated and uncoated silicon carbide plates. *Journal of Applied Physics*, 112(2):024304, 2012.
- [33] Philippe Ben-Abdallah and Svend-Age Biehs. Contactless heat flux control with photonic devices. *AIP Advances*, 5(5):053502, 2015.
- [34] Jiadong Shen, Xianglei Liu, Huan He, Weitao Wu, and Baoan Liu. High-performance noncontact thermal diode via asymmetric nanostructures. *Journal of Quantitative Spectroscopy and Radiative Transfer*, 211:1–8, 2018.
- [35] Cz Marucha, J Mucha, and J Rafałowicz. Heat flow rectification in inhomogeneous gaas. *physica status solidi (a)*, 31(1):269–273, 1975.
- [36] Heinrich Hoff. Asymmetrical heat conduction in inhomogeneous materials. *Physica A: Statistical Mechanics and its Applications*, 131(2):449–464, 1985.
- [37] Xin Sun, Shigeo Kotake, Yasuyuki Suzuki, and Masafumi Senoo. Evalua-

- tion of thermal rectification at the interface of dissimilar solids by phonon heat transfer. *Heat Transfer—Asian Research: Co-sponsored by the Society of Chemical Engineers of Japan and the Heat Transfer Division of ASME*, 30(2):164–173, 2001.
- [38] David B Go and Mihir Sen. On the condition for thermal rectification using bulk materials. *Journal of heat transfer*, 132(12), 2010.
- [39] Jiuning Hu, Xiulin Ruan, and Yong P Chen. Thermal conductivity and thermal rectification in graphene nanoribbons: a molecular dynamics study. *Nano letters*, 9(7):2730–2735, 2009.
- [40] Xueming Yang, Jiangxin Xu, Sihan Wu, Dapeng Yu, and Bingyang Cao. The effect of structural asymmetry on thermal rectification in nanostructures. *Journal of Physics: Condensed Matter*, 30(43):435305, 2018.
- [41] Yan Wang, Ajit Vallabhaneni, Jiuning Hu, Bo Qiu, Yong P Chen, and Xiulin Ruan. Phonon lateral confinement enables thermal rectification in asymmetric single-material nanostructures. *Nano letters*, 14(2):592–596, 2014.
- [42] Jonghoon Lee, Vikas Varshney, Ajit K Roy, John B Ferguson, and Barry L Farmer. Thermal rectification in three-dimensional asymmetric nanostructure. *Nano letters*, 12(7):3491–3496, 2012.
- [43] C. W. Chang, D. Okawa, A. Majumdar, and A. Zettl. Solid-state thermal rectifier. *Science*, 314(5802):1121–1124, 2006.
- [44] Dvira Segal. Single mode heat rectifier: Controlling energy flow between electronic conductors. *Physical review letters*, 100(10):105901, 2008.
- [45] M. J. Martínez-Pérez and F. Giazotto. Efficient phase-tunable Josephson thermal rectifier. *Applied Physics Letters*, 102(18):182602, 2013.
- [46] F Giazotto and FS Bergeret. Thermal rectification of electrons in hybrid normal metal-superconductor nanojunctions. *Applied Physics Letters*, 103(24):242602, 2013.
- [47] Gabriel T Landi, E Novais, Mário J de Oliveira, and Dragi Karevski. Flux rectification in the quantum x x z chain. *Physical Review E*, 90(4):042142, 2014.
- [48] R. Scheibner, M. König, D. Reuter, A. D. Wieck, C. Gould, H. Buhmann, and L. W. Molenkamp. Quantum dot as thermal rectifier. *New Journal of Physics*, 10(8):083016, 2008.
- [49] Jorden Senior, Azat Gubaydullin, Bayan Karimi, Joonas T Peltonen,

- Joachim Ankerhold, and Jukka P Pekola. Heat rectification via a superconducting artificial atom. *Communications Physics*, 3(1):1–5, 2020.
- [50] Tomi Ruokola, Teemu Ojanen, and Antti-Pekka Jauho. Thermal rectification in nonlinear quantum circuits. *Physical Review B*, 79(14):144306, 2009.
- [51] L. P. Wang and Z. M. Zhang. Thermal rectification enabled by near-field radiative heat transfer between intrinsic silicon and a dissimilar material. *Nanoscale and Microscale Thermophysical Engineering*, 17(4):337–348, 2013.
- [52] Shizheng Wen, Xianglei Liu, Sheng Cheng, Zhoubing Wang, Shenghao Zhang, and Chunzhuo Dang. Ultrahigh thermal rectification based on near-field thermal radiation between dissimilar nanoparticles. *Journal of Quantitative Spectroscopy and Radiative Transfer*, 234:1–9, 2019.
- [53] Soumyadipta Basu and Mathieu Francoeur. Near-field radiative transfer based thermal rectification using doped silicon. *Applied Physics Letters*, 98(11):113106, 2011.
- [54] Linxiao Zhu, Clayton R Otey, and Shanhui Fan. Ultrahigh-contrast and large-bandwidth thermal rectification in near-field electromagnetic thermal transfer between nanoparticles. *Physical Review B*, 88(18):184301, 2013.
- [55] Karl Joulain, Younes Ezzahri, Jérémie Drevillon, Benoit Rousseau, and Domingos De Sousa Meneses. Radiative thermal rectification between SiC and SiO₂. *Optics express*, 23(24):A1388–A1397, 2015.
- [56] Guoding Xu, Jian Sun, Hongmin Mao, and Tao Pan. Highly efficient near-field thermal rectification between insb and graphene-coated sio₂. *Journal of Quantitative Spectroscopy and Radiative Transfer*, 220:140–147, 2018.
- [57] Alok Ghanekar, Jun Ji, and Yi Zheng. High-rectification near-field thermal diode using phase change periodic nanostructure. *Applied Physics Letters*, 109(12):123106, 2016.
- [58] Zhiheng Zheng, Xianglei Liu, Ao Wang, and Yimin Xuan. Graphene-assisted near-field radiative thermal rectifier based on phase transition of vanadium dioxide (vo₂). *International Journal of Heat and Mass Transfer*, 109:63–72, 2017.
- [59] Anthony Fiorino, Dakotah Thompson, Linxiao Zhu, Rohith Mittapally, Svend-Age Biehs, Odile Bezenenet, Nadia El-Bondry, Shailendra Bansropun, Philippe Ben-Abdallah, Edgar Meyhofer, et al. A thermal diode based on nanoscale thermal radiation. *ACS nano*, 12(6):5774–5779, 2018.

- [60] Wei Gu, Gui-Hua Tang, and Wen-Quan Tao. Thermal switch and thermal rectification enabled by near-field radiative heat transfer between three slabs. *International Journal of Heat and Mass Transfer*, 82:429–434, 2015.
- [61] Jinguo Huang, Qiang Li, Zhiheng Zheng, and Yimin Xuan. Thermal rectification based on thermochromic materials. *International Journal of Heat and Mass Transfer*, 67:575–580, 2013.
- [62] Raphael St-Gelais, Biswajeet Guha, Linxiao Zhu, Shanhui Fan, and Michal Lipson. Demonstration of strong near-field radiative heat transfer between integrated nanostructures. *Nano letters*, 14(12):6971–6975, 2014.
- [63] Jiadong Shen, Xianglei Liu, and Yimin Xuan. Near-field thermal radiation between nanostructures of natural anisotropic material. *Physical Review Applied*, 10(3):034029, 2018.
- [64] Cheng-Long Zhou, Yong Zharig, Hong-Liang Yi, and Lei Qu. Radiation-based near-field thermal rectification via asymmetric nanostructures of the single material. In *2019 Photonics & Electromagnetics Research Symposium-Spring (PIERS-Spring)*, pages 2652–2658. IEEE, 2019.
- [65] Elyes Nefzaoui, Karl Joulain, Jérémie Drevillon, and Younès Ezzahri. Radiative thermal rectification using superconducting materials. *Applied Physics Letters*, 104(10):103905, 2014.
- [66] Elyes Nefzaoui, Jérémie Drevillon, Younès Ezzahri, and Karl Joulain. Simple far-field radiative thermal rectifier using Fabry–Perot cavities based infrared selective emitters. *Applied optics*, 53(16):3479–3485, 2014.
- [67] Romil Audhkhasi and Michelle L Povinelli. Design of far-field thermal rectifiers using gold–vanadium dioxide micro-gratings. *Journal of Applied Physics*, 126(6):063106, 2019.
- [68] Kota Ito, Kazutaka Nishikawa, Hideo Iizuka, and Hiroshi Toshiyoshi. Experimental investigation of radiative thermal rectifier using vanadium dioxide. *Applied Physics Letters*, 105(25):253503, 2014.
- [69] Shichao Jia, Yang Fu, Yishu Su, and Yungui Ma. Far-field radiative thermal rectifier based on nanostructures with vanadium dioxide. *Optics letters*, 43(22):5619–5622, 2018.
- [70] Alok Ghanekar, Gang Xiao, and Yi Zheng. High contrast far-field radiative thermal diode. *Scientific reports*, 7(1):1–7, 2017.
- [71] Hugo Prod’homme, Younès Ezzahri, Jérémie Drevillon, and Karl Joulain. Dynamical behaviour of a far-field radiative thermal transistor. In *2015 21st International Workshop on Thermal Investigations of ICs and Sys-*

- tems (THERMINIC)*, pages 1–4. IEEE, 2015.
- [72] Jose Ordonez-Miranda, Younès Ezzahri, Jose A. Tiburcio-Moreno, Karl Joulain, and Jérémie Drevillon. Radiative thermal memristor. *Phys. Rev. Lett.*, 123:025901, Jul 2019. doi: 10.1103/PhysRevLett.123.025901. URL <https://link.aps.org/doi/10.1103/PhysRevLett.123.025901>.
 - [73] PJ Van Zwol, Karl Joulain, Philippe Ben-Abdallah, and Joël Chevrier. Phonon polaritons enhance near-field thermal transfer across the phase transition of vo 2. *Physical Review B*, 84(16):161413, 2011.
 - [74] D Sawaki, W Kobayashi, Y Moritomo, and I Terasaki. Thermal rectification in bulk materials with asymmetric shape. *Applied Physics Letters*, 98(8):081915, 2011.
 - [75] Michael F Modest. *Radiative heat transfer*. Academic press, 2013.
 - [76] S. N. Bose. Planck’s law and light quantum hypothesis. *Z. Phys*, 26(1):178, 1924.
 - [77] Edward D. Palik. *Handbook of Optical Constants of Solids, Five-Volume Set: Handbook of Thermo-Optic Coefficients of Optical Materials with Applications*. Elsevier, 1997.
 - [78] Marvin J Weber. *Handbook of optical materials*, volume 19. CRC press, 2002.
 - [79] A. Beran. The reflectance behaviour of gold at temperatures up to 500° C. *Tschermaks mineralogische und petrographische Mitteilungen*, 34(3-4):211–215, 1985.
 - [80] L. N. Aksyutov. Temperature dependence of the optical constants of tungsten and gold. *Journal of Applied Spectroscopy*, 26(5):656–660, 1977.
 - [81] Kikuo Ujihara. Reflectivity of metals at high temperatures. *Journal of Applied Physics*, 43(5):2376–2383, 1972.
 - [82] J. W. C. De Vries. Temperature and thickness dependence of the resistivity of thin polycrystalline aluminium, cobalt, nickel, palladium, silver and gold films. *Thin Solid Films*, 167(1-2):25–32, 1988.
 - [83] BW Veal and AP Paulikas. Optical properties of molybdenum. i. experiment and kramers-kronig analysis. *Physical Review B*, 10(4):1280, 1974.
 - [84] HRPH Ehrenreich and HR Philipp. Optical properties of ag and cu. *Physical Review*, 128(4):1622, 1962.
 - [85] I Setién-Fernández, T Echániz, L González-Fernández, RB Pérez-Sáez,

- and MJ Tello. Spectral emissivity of copper and nickel in the mid-infrared range between 250 and 900 c. *International Journal of Heat and Mass Transfer*, 71:549–554, 2014.
- [86] Leo Esaki. Properties of thermally treated germanium. *Physical Review*, 89(5):1026, 1953.
- [87] Thomas R Harris. *Optical properties of Si, Ge, GaAs, GaSb, InAs, and InP at elevated temperatures*. PhD thesis, Air Force Institute of Technology, 2010.
- [88] Daniel Ng. Temperature-dependent reflectivity of silicon carbide. Technical report, NASA Lewis Research Center, 02 1992.
- [89] Karly M. Pitman, Angela K. Speck, Anne M. Hofmeister, and Adrian B. Corman. Optical properties and applications of silicon carbide in astrophysics. In *Silicon Carbide-Materials, Processing and Applications in Electronic Devices*. InTech, 2011.
- [90] Daniel C. Harris, Meghan Baronowski, Ladd Henneman, Leonard V. LaCroix, Clyde Wilson, Shelby C. Kurzius, Bob Burns, Keith Kitagawa, Jozef Gembarovic, and Steven M. Goodrich. Thermal, structural, and optical properties of Cleartran® multispectral zinc sulfide. *Optical Engineering*, 47(11):114001, 2008.
- [91] Yu-Bin Chen and ZM Zhang. Heavily doped silicon complex gratings as wavelength-selective absorbing surfaces. *Journal of Physics D: Applied Physics*, 41(9):095406, 2008.
- [92] Soumyadipta Basu and Liping Wang. Near-field radiative heat transfer between doped silicon nanowire arrays. *Applied Physics Letters*, 102(5):053101, 2013.
- [93] HH Li. Refractive index of silicon and germanium and its wavelength and temperature derivatives. *Journal of Physical and Chemical Reference Data*, 9(3):561–658, 1980.
- [94] T Skauli, PS Kuo, KL Vodopyanov, TJ Pinguet, O Levi, LA Eyres, JS Harris, MM Fejer, B Gerard, L Becouarn, et al. Improved dispersion relations for gaas and applications to nonlinear optics. *Journal of Applied Physics*, 94(10):6447–6455, 2003.
- [95] Glen D Gillen, Chris DiRocco, Peter Powers, and Shekhar Guha. Temperature-dependent refractive index measurements of wafer-shaped inas and insb. *Applied optics*, 47(2):164–168, 2008.
- [96] Mario Bertolotti, Victor Bogdanov, Aldo Ferrari, Andrei Jascow, Natalia

- Nazorova, Alexander Pikhtin, and Luigi Schirone. Temperature dependence of the refractive index in semiconductors. *JOSA B*, 7(6):918–922, 1990.
- [97] HH Li. Refractive index of zns, znse, and znfe and its wavelength and temperature derivatives. *Journal of physical and chemical reference data*, 13(1):103–150, 1984.
- [98] Douglas B Leviton and Bradley J Frey. Temperature-dependent refractive index of cleartran zns to cryogenic temperatures. In *Cryogenic Optical Systems and Instruments 2013*, volume 8863, page 886307. International Society for Optics and Photonics, 2013.
- [99] Gary Hawkins and Roger Hunneman. The temperature-dependent spectral properties of filter substrate materials in the far-infrared (6–40 μm). *Infrared physics & technology*, 45(1):69–79, 2004.
- [100] G. G. Macfarlane, T. P. McLean, J. E. Quarrington, and V. Roberts. Fine structure in the absorption-edge spectrum of Ge. *Physical Review*, 108(6):1377, 1957.
- [101] W. G. Spitzer, D. Kleinman, and D. Walsh. Infrared properties of hexagonal silicon carbide. *Physical Review*, 113(1):127, 1959.
- [102] W. G. Spitzer, D. A. Kleinman, and C. J. Frosch. Infrared properties of cubic silicon carbide films. *Physical Review*, 113(1):133, 1959.
- [103] Craig F. Bohren and Donald R. Huffman. *Absorption and scattering of light by small particles*. John Wiley & Sons, 2008.
- [104] H. Mutschke, A. C. Andersen, D. Clément, Th Henning, and G. Peiter. Infrared properties of SiC particles. *arXiv preprint astro-ph/9903031*, 1999.
- [105] D. Clément, H. Mutschke, R. Klein, and Th Henning. New laboratory spectra of isolated beta-SiC nanoparticles: Comparison with spectra taken by the Infrared Space Observatory. *The Astrophysical Journal*, 594(1):642, 2003.
- [106] Claus P Cagran, Leonard M Hanssen, Mart Noorma, Alex V Gura, and Sergey N Mekhontsev. Temperature-resolved infrared spectral emissivity of sic and pt-10rh for temperatures up to 900° c. *International Journal of Thermophysics*, 28(2):581–597, 2007.
- [107] P.J.L Herve and L.K.J Vandamme. Empirical temperature dependence of the refractive index of semiconductors. *Journal of Applied Physics*, 77(10):5476–5477, 1995.

Supplementary Materials I: Radiative properties extraction of considered materials

Table 2: Available data of considered materials

Materials	Reflectivity(ρ)	Transmittivity(t)	Emissivity(ϵ)
Ge	[93]	[87]	$\epsilon=1-\rho-t$
GaAs	[94, 95]	[87]	$\epsilon=1-\rho-t$
GaSb	[107]	[87]	$\epsilon=1-\rho-t$
InAs	[95, 96]	[87]	$\epsilon=1-\rho-t$
ZnS	[90, 97–99]	[90]	[90]
SiC	$\rho=1-\epsilon$	opaque sample[106]	[106]
Au	[80]	opaque sample[80]	$\epsilon=1-\rho$
Cu	[85]	opaque sample[85]	[85]

Radiative optical properties sourced from the works cited in this paper, have provided all the necessary temperature dependent data as is required in this study. Table 2 delineates from which reference the sample radiative optical properties have been gathered and how a particular material property, if not available, of each sample has been calculated. Here, recalling the notations in section 2.1, $\epsilon(\lambda, T)$, $\rho(\lambda, T)$ and $t(\lambda, T)$ are the material emissivity, reflectivity and transmittivity respectively.

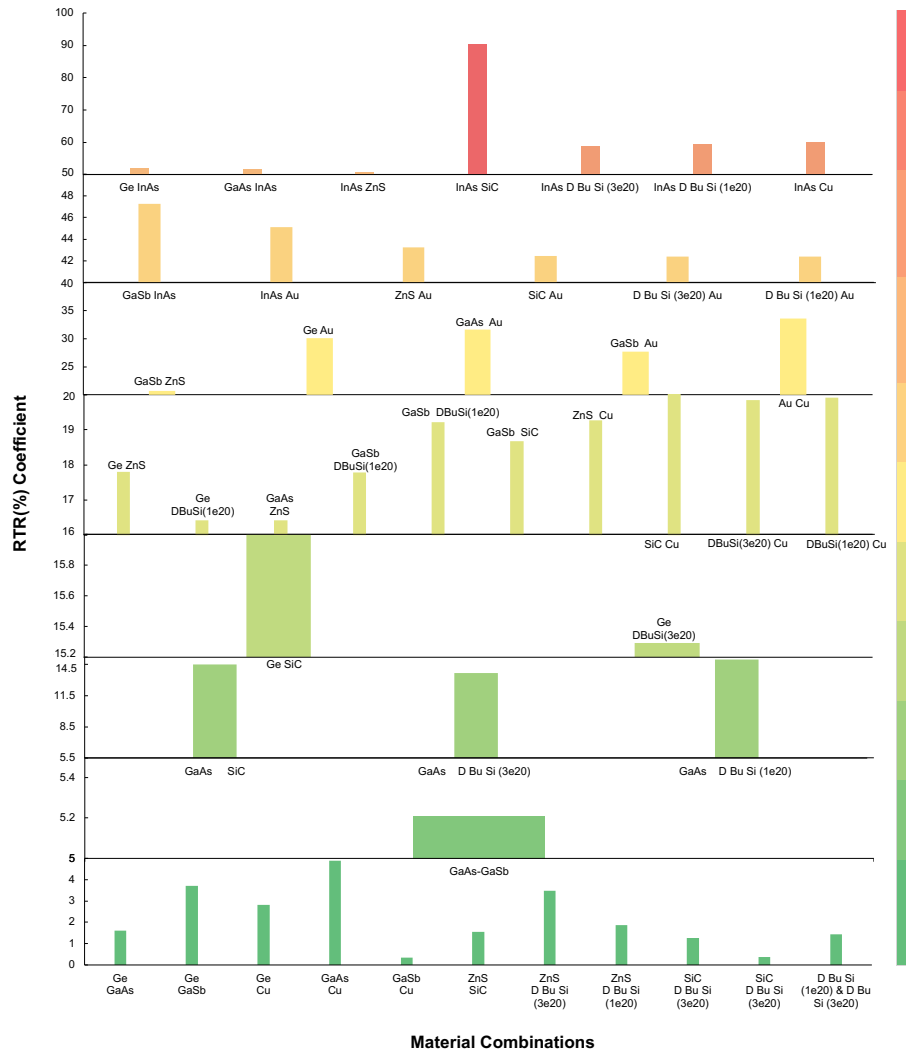


Figure 7: Mapping RTR coefficients of thermal rectifiers made of pairs of considered materials for a thermal bias of 200 K based on the table in Fig.4

Supplementary Materials II: Mapping RTR coefficient of considered materials

As depicted in Table 4, RTR coefficients for different combinations of considered materials, belong to different ranges from 0-91%. In an attempt to streamline and to make each material combination identifiable for an appropriate RTR coefficient, all RTR coefficients are mapped in Figure7 in different

ranges namely: 0-5%, 5-5.5%, 5.5-15.2%, 15.2-16%, 16-20%, 20-40%, 40-50%, 50-100%. These ranges have been ascertained relying on the overall data range in Table 4. Each bar height represents the value of the RTR coefficient and the bar width represents the distribution of entries for each data range. The bar color map corresponds to the amplitude of RTR i.e the lowest values starting from green to red being the highest value obtained. As seen in Figure7, there are highest no of entries in the range from 16-20% and 0-5%. There are 7 material combinations in the range of 50-100%, which suggests that these combinations have non negligible thermal rectification.